PHOTODEGRADATION OF ACETYLSALICYLIC ACID UNDER SOLAR RADIATION USING ZnO/$BaSnO_3$ AS A PHOTOCATALYST

Flavio H. C. Boldrin[1], Laila G. Andrade[1], Ikaro Tessaro[1], Cesar A. F. M. P. Lico[1], Lucas H. Cardia[1] Bruno H. B. Silva[1], Paula M. R. M. Santos[1], Luiza F. Pinheiro[1], Nicolas P. Moraes[2] & Liana A. Rodrigues[1]*

[1]Escola de Engenharia de Lorena-EEL/USP, Estrada Municipal do Campinho S/N, CEP 12602-810, Lorena, São Paulo, Brazil.
[2]São Carlos Institute of Chemistry, University of São Paulo, Av. Trab. São Carlense, 400 - Parque Arnold Schimidt, São Carlos - SP, 13566-590
** Corresponding author's email address: liana.r@usp.br*

ABSTRACT

In the realm of environmental biotechnology, the detection and degradation of emerging micropollutants through advanced oxidative processes are proving to be promising and necessary. In this study, the efficiency of acetylsalicylic acid (ASA) photodegradation under sunlight radiation using ZnO/$BaSnO_3$ as a photocatalyst was evaluated. Characterizations by X-ray diffraction (XRD) and infrared spectroscopy confirmed the presence of ZnO and $BaSnO_3$ in the binary composite, as well as in their respective unary forms. Additionally, diffuse reflectance spectroscopy (DRS) analysis of the materials demonstrated good absorption capacity at shorter wavelengths, as well as low activity at wavelengths greater than 420 nm. Furthermore, from the DRS data analysis, bandgaps of 3.12 eV, 3.18 eV, and 3.22 eV were determined for BaSnO3, ZnO, and ZnO/$BaSnO_3$, respectively. Finally, it was confirmed that ZnO/$BaSnO_3$ exhibited the highest efficiency in ASA degradation, degrading 73.5% of the initial solution under sunlight radiation over a period of 5 hours, indicating the possible formation of efficient heterojunctions between ZnO and BaSnO3 in the binary composite.

Keywords: Acetylsalicylic acid. Photocatalysis. ZnO. $BaSnO_3$.

1 INTRODUCTION

Various classes of emerging pollutants (EPs) have garnered global research interest due to their negative environmental effects and the difficulty of their remediation, as they are recalcitrant to traditional water and wastewater treatment methods[1-3]. Acetylsalicylic acid (ASA), an EP categorized within pharmaceuticals and personal care products, is of particular concern due to its recalcitrant nature, ease of acquisition, and high availability, leading to significant bioaccumulation and potential adverse effects on the flora and fauna it contacts[4].

In the sphere of environmental biotechnology, the importance of advanced methods to detect and degrade emerging micropollutants is being increasingly recognized[2,3]. Advanced oxidative processes have surfaced as a promising strategy to confront environmental pollution issues. These methods enhance the efficiency of removing and degrading persistent substances and advocate for more effective waste management practices, adhering to environmental conservation and public safety principles[4]. Heterogeneous photocatalysis is a promising method for the remediation of this pharmaceutical, demonstrating high efficiency in the degradation and mineralization of various EPs[5]. In this technique, photocatalysts are irradiated with light, which excites electrons from the valence band (VB) to the semiconductors' conduction band (CB). The vacancy in the VB and the electron in the CB generate active radicals in an aqueous medium, which are precursors for the degradation reactions of pollutants[6].

ZnO stands out among commonly used photocatalysts due to its non-toxicity, good absorption in the UV spectrum, and facile synthesis. However, the high recombination rate of electron-hole pairs in this semiconductor reduces the efficiency of active radical generation in aqueous media, as well as its photocorrosion under UV radiation and low activation in the visible spectrum leads to the necessity for the development of more efficient materials. Heterojunction engineering offers a promising alternative to address these issues, as the interaction between semiconductors can optimize electron transfer mechanisms, reduce recombination rates, and potentially enhance photocatalytic activity at longer wavelengths, thereby making the photocatalytic process more viable[7].

Perovskite $BaSnO_3$ is a promising candidate for forming efficient heterojunctions with ZnO due to its suitable band configuration, non-toxicity, and good activation under UV radiation[8]. Therefore, this study aims to evaluate the photocatalytic efficiency of the ZnO/$BaSnO_3$ binary system compared to its corresponding unary components (ZnO and $BaSnO_3$) in the degradation of ASA under sunlight radiation.

2 MATERIAL & METHODS

The synthesis of $BaSnO_3$ was initiated by dissolving pre-defined quantities of $Ba(NO_3)_2$ and $SnCl_2{\cdot}6H_2O$ in separate portions of 50 ml deionized water. After mixing the solutions and adding NaOH (3 g in 50ml deionized water), the resulting $BaSnO_3$ precursor was allowed to precipitate over 24 hours, followed by filtration, washing, drying, grinding, sieving, and calcination at 900°C for 3h in a tubular furnace. Similarly, ZnO was synthesized by precipitating 17.76 g $Zn(NO_3)_2.6H_2O$ in 50 ml deionized water with 7.26 g KOH in 50 ml deionized water, with subsequent filtration, washing, drying, grinding, sieving, and calcination at 600°C for 0,5h in a muffle furnace in a N_2 atmosphere. The ZnO/$BaSnO_3$ binary compound was prepared by solubilizing 17.76 g $Zn(NO_3)_2.6H_2O$

and dispersing 0.255 g of previously prepared $BaSnO_3$ in 50 ml deionized water, followed by precipitation and identical post-treatment steps as ZnO.

Following synthesis, the crystalline structure, chemical composition, optical properties, and bandgaps of the materials were analyzed through characterization using X-ray diffraction (DRX), by Fourier-transform infrared spectroscopy (FTIR), and diffuse reflectance spectroscopy (DRS) techniques. For these purposes, a PANalytical Empyrean X-ray equipment operating at 40 kV and 30 mA with a copper tube (CuKα radiation, λ=0.15418 nm), a universal attenuated total reflectance (UATR) accessory on a Perkin Elmer Frontier spectrometer and a Shimadzu UV-2600 spectrophotometer equipped with an ISR2600 Plus integrating sphere were respectively used.

Moreover, the photocatalytic activity of the materials was evaluated using a 0.5 L jacketed reactor maintained at 25°C. Each test involved introducing a 0,5 L solution containing 10 mg L^{-1} acetylsalicylic acid and 0.1 g of the photocatalyst into the reactor. The pollutant concentration was monitored using a Shimadzu UV-visible spectrophotometer at a wavelength of 226 nm. Samples were withdrawn at regular 15-minute intervals under dark conditions until adsorption-desorption equilibrium was reached, after which the Osram ultra-vitalux 300 W lamp for sunlight radiation was activated. Samples were then collected at regular 15-minute intervals defined intervals for the first hour and 30-minute intervals until 5 hours of degradation or until complete pollutant degradation. Photocatalytic efficiency was determined using *Equation 1*:

$$Degradation\ efficiency\ (\%) = \frac{C_0 - C}{C_0} * 100 \quad (1)$$

Where: C_0 represents the initial pollutant concentration of the reaction mixture; C represents the concentration at a given sample collection time.

3 RESULTS & DISCUSSION

Figures 1A, B, and C show, respectively, the results obtained for the characterization of the materials by XRD, FTIR, and DRS.

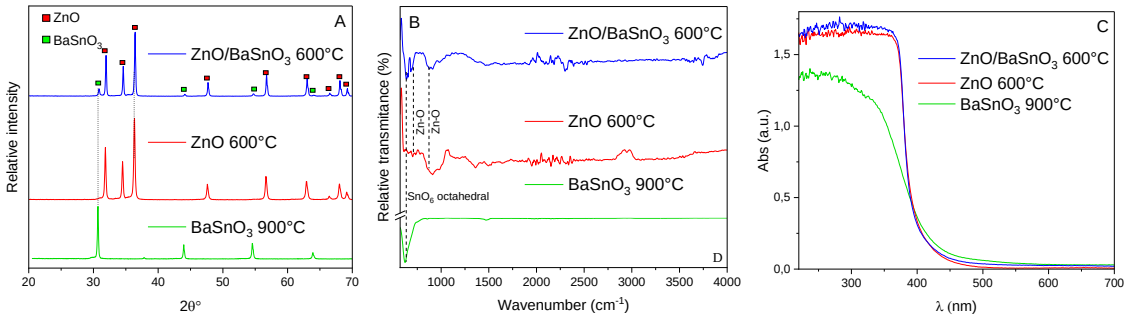

Figure 1 - DRX (A), FTIR (B) and DR (C) for the materials

According to *Figure 1A*, the presence of representative peaks of the hexagonal wurtzite crystalline structure of ZnO (JCPDS 36-1451) and cubic perovskite of $BaSnO_3$ (JCPDS 15-0708) was confirmed for the respective unary materials and peaks from both structures are also evident in the results for the binary ZnO/$BaSnO_3$, demonstrating the efficiency of the synthesis routes used[9,10]. Additionally, a slight shift to higher wavelengths of the peaks related to ZnO in the binary compared to the unary was observed, which can be explained by the possible distortion of the ZnO crystalline structure due to the insertion of $BaSnO_3$.

Similarly, the infrared spectroscopy analyses shown in *Figure 1B* also confirmed the presence of ZnO and $BaSnO_3$ in the respective desired materials. The band at 645 cm^{-1} found for $BaSnO_3$ and ZnO/$BaSnO_3$ can be related to the stretching vibrations of the {SnO6}-octahedron[11], and the bands at 720 and 905 cm^{-1} observed for ZnO and ZnO/$BaSnO_3$ are related to Zn-O bonds[12].

Furthermore, regarding *Figure 1C*, the absorption profile of the materials between 250 and 700 nm can be observed. As expected, although slightly better than ZnO, the absorption capacity of $BaSnO_3$ was low at wavelengths above 420 nm[13,14]. The small absorption capacity still observed for ZnO up to 500 nm, although counterintuitive relative to the literature, can be explained by the presence of oxygen vacancies, leading to isolated defects below the ZnO conduction band, which may result in higher photocatalytic activity in this wavelength range[15]. Finally, for ZnO/$BaSnO_3$, results similar to ZnO were observed, with a slight improvement in absorption capacity for wavelengths above 420 nm, indicating a possible positive effect of the addition of $BaSnO_3$ to the structure.

Moreover, from the data shown in *Figure 1C*, the bandgaps of the tested materials were determined. For this pupose, a model proposed in the literature was used[16], and the bandgaps found were 3.12 eV, 3.18 eV, and 3.21 eV for $BaSnO_3$, ZnO, and ZnO/$BaSnO_3$ respectively. The results for the unary materials agree with reported values[17,18], and the bandgap of the binary material is consistent with expectations, being similar to that observed for ZnO[15].

After characterization analysis, the photocatalytic activity of the materials under sunlight radiation for the degradation of AAS was evaluated, as shown in *Figure 2*.

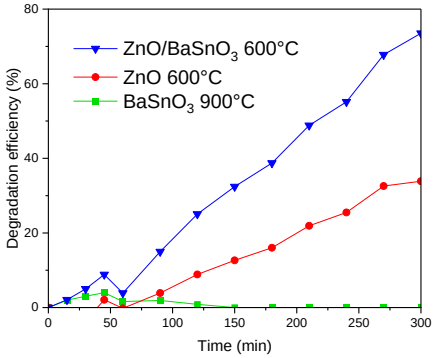

Figure 2 - Degradation efficiency of ASA under sunlight radiation for the binary ZnO/$BaSnO_3$ and its unary counterparts ZnO and $BaSnO_3$

Upon examining *Figure 2*, it becomes evident that the binary material outperforms the unary counterparts, displaying a 73.5% degradation efficiency of ASA after 5 hours of reaction. This outcome is likely attributed to the formation of an efficient heterojunction between ZnO and $BaSnO_3$, facilitating superior electron-hole separation, thereby diminishing the recombination rate and consequently enhancing photocatalytic activity. The subdued activity of $BaSnO_3$ is attributable to its elevated recombination rate and limited sensitization to longer wavelengths[19]. Conversely, ZnO exhibits intermediate activity, aligning with the DRS findings in *Figure 1C*, showcasing heightened absorption compared to $BaSnO_3$ at shorter wavelengths (predominantly in the UV region) and marginal absorption between 400 and 500 nm. This behavior stems from the creation of an isolated defect state beneath the conduction band of ZnO, potentially enabling activity within this wavelength range[15].

4 CONCLUSION

Initially, the effectiveness of the synthesis routes employed for ZnO, $BaSnO_3$, and ZnO/$BaSnO_3$ was validated through XRD and FTIR characterizations. Furthermore, DRS analyses indicated robust absorption of the materials at shorter wavelengths and minimal absorption beyond 420 nm. Moreover, DRS measurements enabled the determination of bandgaps, revealing values of 3.12 eV, 3.18 eV, and 3.22 eV for $BaSnO_3$, ZnO, and ZnO/$BaSnO_3$, respectively. Subsequent photocatalytic activity assessments underscored the superior performance of ZnO/$BaSnO_3$ over the unary materials, achieving a notable 73.5% degradation of AAS under sunlight radiation. This enhanced activity is likely attributable to the establishment of efficient heterojunctions between the oxides, leading to a reduced recombination rate and thereby facilitating improved charge separation.

REFERENCES

1 LIU, T. ANIAGOR, C. O. EJIMOFOR, M. I. MENKITI, M. C. TANG, K. H. D. CHIN, B. L. F. CHAN, Y. H. YIIN, C. L. CHEAH,K. W. HO CHAI, Y. LOCK, S. S. M. YAP, K. L. WEE, M. X. J. YAP, P.-S. 2023. Mol. Liq. J. 374. 121144.

2 KAVITHA, 2022. Results Eng. 14. 100469.

3 STAMATIS, N. K. KONSTANTINOU, I. K. J. 2013. Environ. Sci. Heal. - Part B Pestic. Food Contam. Agric. Wastes. 48. 800–813.

4 NORDIN, A. H. ABDUL SAMAD, N. PAIMAN, S. H. MD NOOR, S. F. RUSHDAN, A. I. NGADI, N. 2024. Mater. Today Proc. 96. 30-34.

5 MOHAN, H. YOO, S. THIMMARAYAN, S. OH, H. S. KIM, G. SERALATHAN, K.-K. SHIN, T. 2021. Environ. Pollut. 289. 117864.

6 LI, X. BAI, Y. SHI, X. SU, N. NIE, G. ZHANG, R. NIE, H. YE, L. 2021. Mater. Adv. 2. 1570–1594.

7 SOUSA, J. G. M. de SILVA, T. V. C. da MORAES, N. P. de SILVA, M. L. C. P. da ROCHA, R. S. LANDERS, R. RODRIGUES, L. A. 2020. Mater. Chem. Phys. 256. 123651.

8 LI, T. JIANG, A. DI, Y. ZHANG, D. ZHU, X. DENG, L. DING, X. CHEN, S. 2021. Chem. Sel. 6. 10817–10826.

9 PAL, S. SANKAR DAS, N. DAS, B. KUMAR DAS, B. MUKHOPADHYAY, S. KUMAR CHATTOPADHYAY, K. 2020. Appl. Surf. Sci. 530. 147102.

10 ŠARIĆ, A. VRANKIĆ, M. LÜTZENKIRCHEN-HECHT, D. DESPOTOVIĆ, I. PETROVIĆ, Ž. DRAŽIĆ, G. ECKELT, F. 2022. Inorg. Chem. 61. 2962–2979.

11 MARIKUTSA, A. RUMYANTSEVA, M. BARANCHIKOV, A. GASKOV, A. 2015. Mater. 8, 6437–6454.

12 MORAES, N. P. de ROCHA, R. S. SIERVO, A. de PRADO, C. C. A. do PAIVA, T. C. B. de CAMPOS, T. M. B. THIM, G. P. LANZA, M. R. V. RODRIGUES, L. A. 2022. Opt. Mater. 128. 112470.

13 MAHMOUD, S. A. FOUAD, O. A. 2015. Sol. Energy Mater. Sol. Cells. 136. 38–43.

14 ASISI JANIFER, M. ANAND, S. JOSEPH PRABAGAR, C. PAULINE, S. 2021. Mater. Today Proc. 47. 2067–2070.

15 GOUVEA, M. E. V. BOLDRIN, F. H. C. SILVA, B. H. B. da PAIVA, L. K. MORAES, N. P. de AGUIAR, L. G. de RODRIGUES, L. A. Chem. Phys. Impact. 8. 100428.

16 GHOBADI, N. 2013. Int. Nano Lett. 3. 1. 2.

17 MORAES, N. P. de CAMPOS, T. M. B. THIM, G. P. SIERVO, A. de LANZA, M. R. V. RODRIGUES, L. A. 2023. Chem. Phys. Impact. 6. 100182.

18 MKHALID, I. A. EL-HOUT, S. I. 2023. J. Taiwan Inst. Chem. Eng. 146. 104896.

19 BAOUM, A. A. ISMAIL, A. A. 2023. Ceram. Int. 49. 23227–23237.

ACKNOWLEDGEMENTS

The authors would like to thank the Coordenação de Aperfeiçoamento de Pessoal de Nivel Superior (CAPES) - Financing Code 001, and the São Paulo Research Foundation (FAPESP) - Processes n° 2022/04058-2 and 2023/13127-0 and University of São Paulo (PUB USP Scholarships), for the financial support.